X-ray small angle scattering of the human transferrin protein aggregates

A fractal study

A. Congiu Castellano,* M. Barteri,* A. Bianconi,‡ E. Borghi,* L. Cassiano, M. Castagnola,§ S. Della Longa,‡ and A. La Monaca‖

*Dipartimento di Fisica Universita' "La Sapienza" 00185 Roma; ‡Istituto di Medicina Sperimentale Universita' dell'Aquila, 67100 L'Aquila; §C.N.R. Centro di Studio della Chimica dei Recettori e delle Molecole Biologicamente Attive and Istituto di Chimica Universita' Cattolica del Sacro Cuore 00168 Roma; and ‖INFN Laboratori Nazionali di Frascati, 00044 Frascati, Italy

ABSTRACT X-ray small angle scattering experiments, using a pin hole SAXS camera with Synchrotron radiation source, have been performed to study the conformational changes of lyophilized samples of *Apo-*, *Mono-*, and *Diferric-* human transferrin. We report the experimental evidence that the analysis of the scattered intensity through the fractal theory may give information on the particle size and its variation upon iron binding.

INTRODUCTION

The clustering of small particles into a large randomized object is a commonly occurring phenomenon: in biological systems one finds that heating, cooling, and the lyophilization processes lead to protein aggregation. These effects are influenced by many parameters such as pH and ionic strength. Many theoretical and experimental works show that both structure and surface of proteins are fractals (1–5). However, there is only one study of the fractal nature of the protein clusters. Jossang et al. (6) showed that the cluster of the human IgG, obtained by a heat aggregation, have an effective hydrodynamic radius which can be described by a Smoluchowski aggregation process (7), though refinements of this model could account for the nonspherical shape of clusters containing only few monomers.

We have employed Synchrotron Radiation source and a novel SAXS instrument that allows the investigation of anisotropic ordered materials. The advantages in the use of Synchrotron Radiation for SAXS studies are due to the high incident flux and low angular divergence which give high count rates with good resolution.

We have compared the scattering intensities of the lyophilized samples of *Apo-*, *Mono-*, and *Diferric-* transferrin. The human serum transferrin (MW, 80,000) is a metal binding glycoprotein, whose primary function is the transport of iron in the plasma of vertebrates. At present there is a large interest in the structural modifications of the transferrins upon metal binding. There have been suggestions that serotransferrin may also play a role in the transport of a variety of metal ions such as Zn and Al ions that seem correlated to the pathology of some central nervous diseases (8). Serum transferrin may also have a further role in stimulating the growth of cells that is unrelated to its transport function (9). The crystal structure analysis of *Diferric-* serum rabbit transferrin at 3.3 Å resolution has been reported (10). The molecule has a β α structure consisting of a single polypeptide chain folded into two lobes, each containing some 330 amino acids and a single iron binding site. The shape of each lobe has been described by a prolate ellipsoid of approximate semiaxial dimensions $21 \times 25 \times 35$ Å with the major axes of the N and C lobes running almost antiparallel to one another at an angle of 155°. Each lobe is comprised of two dissimilar domains with the iron binding site situated at the domain interface.

X-ray small angle scattering (11, 12), dielectric dispersion, and viscosity measurements, on water solutions of serum transferrin (13), reveal structural changes that take place upon uptake and release of iron that may involve the opening and closing of the domain cleft. In particular, the molecules in solution become more compact upon iron saturation (characterized by a decrease of the radius of gyration), while exactly the opposite behavior has been observed in the apolactoferrin crystal structure (14) as reported in the discussion section.

The results obtained by means the scattering experiments on the protein in solution arise from an average conformation of the protein rather than from the "static" structure as obtained by single crystal diffraction. The crystallization conditions may stabilize a particular conformation of the molecule where the crystal environment "freezes" one of several accessible conformations for a flexible protein. A similar static conformation could be selected by the lyophilization process. It is worth noting that the structural modification in lyophilized protein is already an open problem involving reversible conformational transitions and dehydration of the polypeptidic chains.

The aim of this study is to find out whether the clusters of a protein, obtained by lyophilization process, may be described as a fractal object and to use such an analysis to probe structural details.

FRACTAL THEORY OF PROTEINS

Several theoretical models have been introduced recently to describe the growth of clusters. In the diffusion

All correspondence should be addressed to A. Congiu Castellano.

0006-3495/93/02/520/05 $2.00

limited aggregation (DLA) model (15), in the diffusion limited cluster aggregation (DLCA) model (16), aggregates of molecules grow by adding one molecule at a time. In two-dimensional computer simulations the fractal dimension, D, near 1.4 and in three dimensions, $D = 1.78$, are found. In experimental situations, the exact nature of the kinetic mechanism and the chemical bonding relevant for the aggregation are not known. The reaction limited cluster aggregation (RLCA) model (17) proposes a realistic growth process, because it is able to interpolate between a purely diffusive and a purely chemical situation. Different values of the fractal exponents found in the experimental results may be explained by a number of different effects that determine the characteristics of the cluster growth (18).

It is worth noting that the protein clusters formed by the addition of diffusing a single molecule are not tightly packed with a constant density, but are rather like a random coil polymer (6). In this case, the radius grows asymptotically and the cluster satisfies the number-radius relation in the form $R_i = r_0 i^b$ (where i is the monomeric molecule) with $b = 1/D$.

On the other side, the model introduced by Stapleton-Helman (1, 5) to describe the fractal dimension in the proteins is a self-avoiding walk (SAW) with massless bonds and has a theoretical dimensionality of 5/3 (19). In computing the fractal dimension of a biopolymer chain, according to Colvin (3), one can count the number of monomers $N(R)$ as a function of a radial distance R from an arbitrary origin and fit $N(R)$ to R^D. For proteins, the x-ray crystallographic coordinates of the alpha carbons are used. The fractal dimension D of the chain can be defined as the scaling exponent of the contour length (length along the chain, proportional to N) with respect to the end-to-end length. The values resulting for 50 proteins studied by Colvin fall among (a) a linear chain, and (b) an unrestricted random walk in three-dimensional spaces. The range of the values is 1.19–1.82 for IGG FAB light (208 monomers) and for agglutinin lectin (164 monomers), respectively. It is also possible to reach the same result ignoring the path of the protein's polypeptide back bone and simply scaling the total mass with respect to the distance in the embedding space. If the average residue mass is assigned to each alpha carbon of the polymer and simply counting all alpha carbons within spheres of radius R, the values change between 1.62 and 2.24.

MATERIALS AND METHODS

Human serum apotransferrin (Sigma Chemical Co., St. Louis, MO) of stated 97% purity was used without further purification.

For the preparation of the *Diferric-* transferrin (FeNTfFeC) iron was added to apotransferrin 0.2 mmol/liter in 0.100 mol/l Hepes, 0.025 mol/l $NaHCO_3$ pH 7.50, using $Fe(NH_4)(SO_4)_2$ 2 mmol/liter in HCl 2 mmol/liter, until the protein reached ~95% of saturation, as described by Thompson et al. (20). The carboxy terminal monoferric transferrin (TfFeC) was prepared by adding the appropriate amount of iron, always as ferric ammonium sulfate, to the protein in 0.100 mol/liter MES, 2 mmol/l $NaHCO_3$, pH 5.5. Urea-PAGE of reaction mixtures revealed that under these conditions the metal binds to the carboxy terminal site. The unbound metal was removed by dialysis against the respective buffers, the samples were liophylized and the powders directly used for the small angle scattering measurements.

The x-ray experiments were carried out at the Frascati wiggler (6-poles $B = 1.85$ T, $Ec = 2.7$ keV) beam line. The SR source was operating at an electron energy of 1.5 GeV with an average electron beam current of 30 mA single bunch. The SR was monochromatized by a Si (111) channel cut single crystal. Data were collected at fixed wavelength $\lambda = 1.54$ Å ($\Delta\lambda/\lambda = 10^{-4}$) with a beam of 0.68×0.51 mm^2 of cross-section and an intensity of $2.4\ 10^7$ ph/s on the sample.

The diffraction apparatus, already described in detail (21, 22), incorporates a gas drift-chamber area position sensitive detector connected to a fast computerized data acquisition system (0.7 MHz) with a real-time graphic display using TDC, CAMAC, VME systems. The drift-chamber area detector has uniform sensitivity of detection, high spatial resolution in both dimensions (X drift and Y delay) of at least 155 μm, and a high count acquisition rate (2×10^{-4} cps/pix). With this setup, it is possible to measure a scattering momentum of the order kmin = 8×10^{-3} Å^{-1}. The SAXS camera was situated at 35 m from the wiggler source; a circularly collimated primary beam of diameter 0.5 mm was obtained using a pin-hole collimator consisting of 0.5 and 0.7 mm diameters made in gold disks, in truncated conical shapes. The beam stop (2 mm width), placed on the entrance window of the detector, is also made of gold and can be moved by remote control for alignment. The detector plane was placed at 500 mm from the specimen to record one half of the symmetric scattering pattern, over 180°, on one side of the equatorial plane. Under these conditions, the relative angular resolution of the camera was $\Delta k/k\text{min} = 0.15$.

The measurements have been carried out in the range $10^{-2} < k$ (Å^{-1}) $< 10^{-1}$ on samples freshly prepared. For each protein, five samples were used and the results here reported are the average values calculated on at least five to seven scattering curves. The total data collection time for a protein was 20 min to allow sufficient statistics.

To confirm the absence of radiation damage after x-ray exposure, suitable amounts of protein were dissolved in a buffer solution and examined using Vis-UV optical spectroscopy.

EXPERIMENTAL RESULTS

From the SAXS pattern of lyophilized samples we have obtained the scattering intensity vs. the scattering vector k (Å^{-1}). In order to analyze our experimental data with the fractal theory, we report the double logarithmic representation of scattering curves (Fig. 1) for the samples of *Apo-*, *Mono-*, and *Diferric-* human transferrin. In this figure it is clear that the scattered intensity is almost linear between the points $k = 1/R$ and $k = 1/r_0$. As it is shown in the figure, it is evident that the values of the upper and lower cutoff reported in Table 1 are different for the three samples. In the region $1/R < k < 1/r_0$ the scattered intensities fall on a straight line with a slope of -1.13 for the apotransferrin, -1.52 for monoferric, and -1.38 for *Diferric-* form. From $k > 1/r_0$ there is another linear regime of the scattered intensities with a slope of -4.01 for the apotransferrin, -4.08 for monoferric, and -3.83 for *Diferric-* form (Table 1).

DISCUSSION

In the SAXS experiment (23) the scattered intensity is separated into two factors $P(k)$ and $S(k)$:

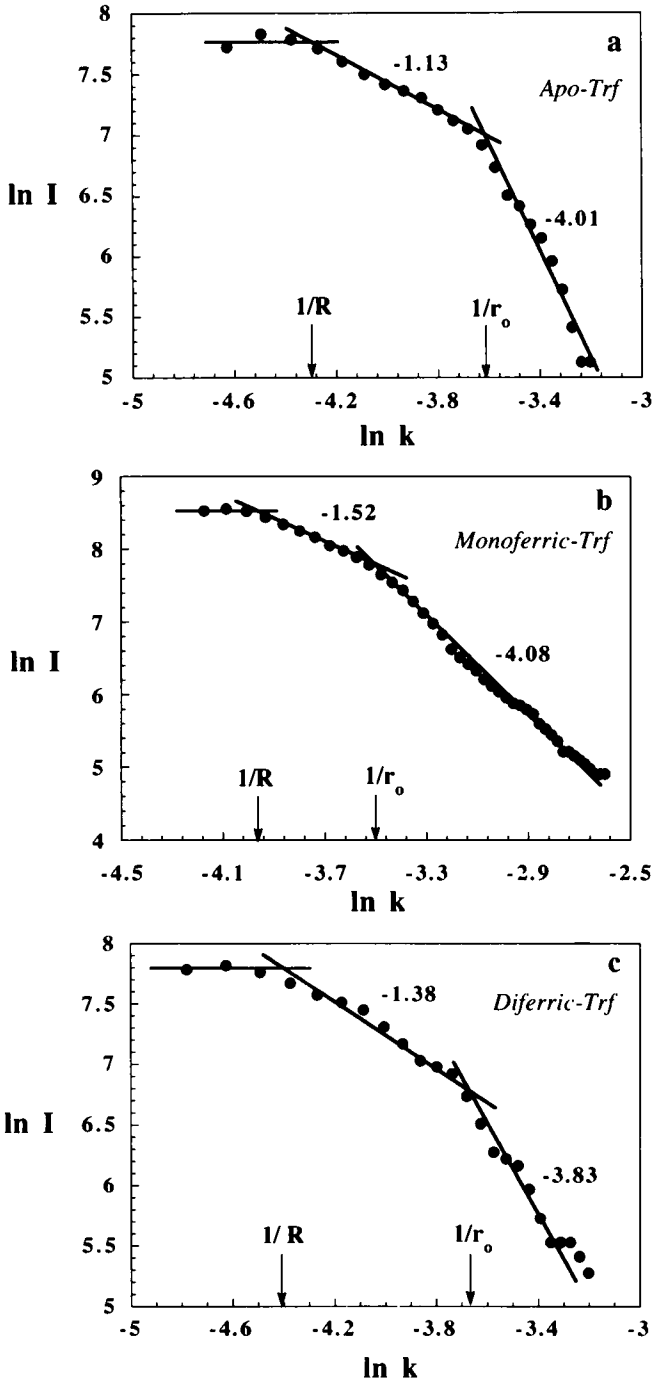

FIGURE 1 Plot ln (I) vs. ln (k) for the lyophilized samples of human *Apo-* transferrin (a), *Mono-* transferrin (b), and *Diferric-* transferrin (c). The arrows indicate the points, where $k = 1/R$ and $k = 1/r_0$. The slopes of the linear regions are reported in Table 2.

$$I(k) = \Phi P(k)\bar{S}(k),$$

where k is the scattering vector defined as

$$k = 4\pi/\lambda \sin \theta/2.$$

$\Phi = N/V$ is the number of individual scatterers in the sample,

$$P(k) = \langle |F(k)|^2 \rangle$$

$$\bar{S}(k) = 1 + \frac{|\langle F(k) \rangle|^2}{\langle |F(k)|^2 \rangle} |S(k) - 1|,$$

where $F(k)$ is the form factor of the particle and $S(k)$ is the interparticle structure factor.

At small k ($kr_0 < 1$), $P(k) \simeq 1$ and $I(k) \simeq \Phi S(k)$, on the contrary at large k ($kr_0 > 1$) $S(k) \simeq 1$ and $I(k) \simeq \Phi P(k)$. One expects then at $k = 1/r_0$ a crossover from a region where $I(k)$ essentially depends on $S(k)$ to a region where $I(k)$ depends on $P(k)$.

In the range $1/R < k < 1/r_0$, where R is the size of the cluster and r_0 is the radius of the monomers that form the fractal cluster, $S(k)$ has the limiting value

$$\lim_{R \to \infty} S(k) = 1 + \text{const}/(kr_0)^D \simeq (kr_0)^{-D}$$

This is a result very often used to analyze the scattered intensity by a fractal object. It is clear that it applies only in an intermediate k region for which both inequalities $kR > 1$ and $kr_0 < 1$ are verified.

At very small k, $S(k)$ must saturate and we have a transition to the so-called Guinier regime. This is because there must be an upper length scale cutoff that reflects the overall size of the system or the length scale at which the cluster density approaches the average density (1). It is necessary to note that the question of small cluster size requires a particular attention since the length scales characterizing the particle diameter and the cluster size may be sufficiently close to make the determination of r_0 and R difficult (24). Our experimental results show that in the range $1/R < k < 1/r_0$, where R is the size of the cluster and r_0 is the radius of the monomers that form the fractal cluster, the scattered intensities fall in a double logarithmic plot on a straight line with a slope of -1.13, -1.38, -1.52 (in the different compounds), which are the fractal dimensions.

For $k > 1/r_0$ there is another linear regime of the scattered intensities with a slope of ~ -4. This slope is the one that is theoretically expected for the monomers that form the fractal structure.

TABLE 1 **Data for apotransferrin and its iron complexes**

	Radii of gyration	Slope for $1/R < k < 1/r_0$	Slope for $k > 1/r_0$
	Å		
Apo-	$R = 77.1 \pm 0.4$ $r_0 = 38.1 \pm 0.4$	−1.13	−4.01
Mono-	$R = 57.7 \pm 0.4$ $r_0 = 32.4 \pm 0.4$	−1.52	−4.08
Diferric-	$R = 83.0 \pm 0.4$ $r_0 = 39.6 \pm 0.4$	−1.38	−3.83

TABLE 2 **Our experimental data of r_0 compared with those of other researchers**

	Syn-rad x-ray scattering (this work)*	Neutron scattering (reference 25)‡	X-ray scattering (reference 11)‡	Syn-rad x-ray scattering (reference 12)‡
	Å	Å	Å	Å
Apo-	38.1 ± 0.4	30.25 ± 0.49	33.0 ± 0.5	32.5 ± 0.2
Mono-	32.4 ± 0.4	—	32.8 ± 0.5	—
Differic-	39.6 ± 0.4	—	31.5 ± 0.5	31.4 ± 0.2

* Samples lyophilized, ‡ in solution.

For large k:

$$(kr_0 > 1)\ P(k) \simeq \frac{9V^2(\rho - \rho_0)^2}{2} \frac{1}{(kr_0)^4}.$$

The experimental result is therefore an indication that the protein remains intact in the aggregate.

The small number of the monomers bounded in the cluster deduced by the values of R and r_0 could have been explained by the aggregation process of the proteins as proposed by Jossang (6). It is well known that only certain relative conformations, orientation and configurations of the protein molecules may lead to the formation of clusters through a number of dipolar and electrostatic interactions. In addition, the cluster may have to overcome a potential barrier, probably including the rupture of a number of weak bonds, before that a stable configuration is reached. This fact may explain why the clusters are formed by only few monomers and why the values of the exponent in the experimental results may be different from the theoretical values.

In Table 2 our experimental data are compared with those of other researchers. While the decrease of the radius of gyration indicates that the molecule of the transferrins in solution seems to be more compact upon saturation with iron, in the lyophilized samples the higher size is observed in the saturated molecule such as in the apolactoferrin crystal structure (12, 14).

The same trend obtained both in the crystalline and in the lyophilized state could be attributed to fact that the protein has a similar static conformation in the two states.

Moreover we observe that while the r_0 value of the *Mono*-ferric transferrin is comparable with those found on water solutions of the transferrins, the gyration radii of the *Apo-* and *Diferric-* lyophilized specimens are higher with respect to those of the samples in solution.

As reported in reference 13, using dielectric dispersion and viscosity measurement, the progressive binding of iron ions determines a remarkable conformational change that involves the opening and closing of the domain cleft, while the hydration value remains high.

This peculiar result could be explained by taking into account that the lyophilization process removes the bulk water (solvent) but the structured water (a few percent of the total) bound in the domain of the protein remains. The conformational structures of the proteins are deeply affected by the presence of these kinds of water, as well as the presence of the solvent, because the water gives an important contribution to the folded structure, by means of hydrophobic, hydrogen bonding, and electrostatic interactions.

Probably, the absence of water in our samples induces a new conformational structure that could give larger values of r_0. The different behavior of the *Monoferric* transferrin could be related to the fact that the molecule is more asymmetric with respect to the *Apo-* and *Diferric*-molecule, and this property perhaps determines the value of the gyration radius.

CONCLUSIONS

The comparison between the experimental results on *Apo-*, *Mono-*, and *Diferric* human transferrin compounds, interpreted by the fractal theory, allows us to distinguish the particle and the cluster size and their contributions to the scattered intensity. Moreover, the experimental data confirms that the iron binding produces conformational changes in the protein molecules in agreement with earlier data.

An extension of these experiments on aggregates of hemocyanins and other proteins is in progress, to probe if the fractal structure is a property ranging from the molecule of a protein up to their clusters.

We are grateful to Dr. A. Vespignani for the helpful discussions and interest during this work.

Received for publication 17 June and in final form 24 September 1992.

REFERENCES

1. Stapleton, H. J., J. P. Allen, C. P. Flynn, D. G. Stinson, and S. R. Kurtz. 1980. Fractal form of proteins. *Phys. Rev. Lett.* 45:1456–1459.
2. Lewis, M., and D. C. Rees. 1985. Fractal surfaces of proteins. *Science (Wash. DC).* 230:1163–1165.
3. Colvin, J. T., and H. J. Stapleton. 1985. Fractal and spectral dimensions of biopolymer chains: solvent studies of electron spin relaxation rates in myoglobin azide. *J. Chem Phys.* 82:4699–4706.
4. MacDonald, M., and N. Jan. 1986. Fractons and fractal dimension of protein. *Can. J. Phys.* 64:1353–1355.

5. Helman, J. S., A. Coniglio, and C. Tsallis. 1984. Fractals and the fractal structure of proteins. *Phys. Rev. Lett.* 53(12):1195–1197.
6. Jossang, T., J. Feder, and E. Rosenquist. 1985. Heat aggregation kinetics of human IgG. *J. Chem. Phys.* 82:574–589.
7. Smoluchowski, M. v. 1916. Drei Vortrage uber Diffusion, Brownsche Molekularbewegung und koagulation von Kolloidteilchen. *Phys. Z.* 17:557–571.
8. Roskams, A. J., and J. R. Connor. 1990. Aluminium access to the brain: a role for transferrin and its receptor. *Proc. Natl. Acad. Sci. USA.* 87:9024–9027.
9. Trowbridge, I. S., and F. Lopez. 1982. Monoclonal antibody to transferrin receptor blocks transferrin binding and inhibits human tumor cell growth in vitro. *Proc. Natl. Acad. Sci. USA.* 79:1175–1179.
10. Bailey, S., R. W. Evans, R. C. Garratt, B. Gorinsky, S. Hasnain, C. Horsburg, H. Jhoti, P. F. Lindley, A. Mydin, R. Sarra, and J. L. Watson. 1988. Molecular structure of serum transferrin at 3.3 Å resolution. *Biochemistry.* 27:5804–5812.
11. Kilar, F., and I. Simon. 1985. The effect of iron binding on the conformation of transferrin. *Biophys. J.* 48:799–802.
12. Grossmann, G. J., M. Neu, E. Pantos, F. J. Schwab, R. W. Evans, E. Townes-Andrews, P. F. Lindley, H. Appel, W. G. Thies, and S. S. Hasnain. 1991. X-ray solution scattering reveals conformational changes upon iron uptake in lactoferrin, serum and ovotransferrin. *Daresbury Lab. Preprint Dl/Sci/P 783E.*
13. Rosseneu-Moutreff, M. Y., F. Soetewey, R. Lamote, and H. Peeters. 1971. Size and shape determination of apotransferrin and transferrin monomers. *Biopolymers.* 10:1039–1048.
14. Anderson, B. F., H. M. Baker, G. e. Norris, S. V. Rumball, and E. N. Baker. 1990. Apolactoferrin structure demonstrates ligand-induced conformational change in transferrins. *Nature (Lond.)* 344:784–787.
15. Meakin, P. 1983. Diffusion-controlled cluster formation in 2-6 dimensional space. *Phys. Rev. A.* 27:1495–1507.
16. Jullien, R., and R. Botet. 1987. Aggregation and fractal aggregates. World Scientific Publishing Co., Singapore. 46–52.
17. Kolb, M., and R. Jullien. 1984. Chemically limited versus diffusion limited aggregation. *J. Phys. Lett.* 45:L977–L981.
18. Sinha, S. K., T. Freltoft, and J. Kiems. 1984. Kinetics of aggregation and gelation. D. P. Landau, and F. Family, editors. North Holland. 87–90.
19. Le Guillou, J. c., and J. Zinn-Justin. 1977. Critical exponents for the n-vector model in three dimensions from field theory. *Phys. Rev. Lett.* 39:95–98.
20. Thompson, C. P., J. K. Grady, and N. D. Chasteen. 1986. The influence of uncoordinated histidines on iron release from transferrin. A chemical modification study. *J. Biol. Chem.* 261:13128–13138.
21. La Monaca, A., M. Barteri, E. Borghi, A. Congiu Castellano, G. Cappuccio, M. Beltramini, B. Salvato, and J. S. Shah. 1991. Application of the improved area detector for continuous small angle scattering using synchrotron radiation. *Nuclear Instruments and Methods in Physics Research A.* 310:403–410.
22. La Monaca, A., M. Barteri, E. Borghi, A. Congiu Castellano, M. Beltramini, B. Salvato, and J. S. Shah. 1991. Advanced small angle x-ray radiation scattering study of hemocyanin oligomers using a high performance two dimensional detector. *Chem. Phys. Lett.* 184:1–4.
23. Teixeira, J. 1986. Experimental methods for studying fractal aggregates. *In* On Growth and Form. H. E. Stanley and N. Ostrow, editors. Martinus Nijhoff Publishers, Dordrecht. 145–162.
24. North, A. N., J. C. Dore, R. K. Heenan, A. R. Mackie, A. M. Howe, B. H. Robinson, and C. Nave. 1988. Small-angle x-ray scattering studies of heterogeneous systems using synchrotron radiation techniques. *Nuclear Instr. Meth. Phys. Res.* B34:188–202.
25. Martel, P., S. M. Kim, and B. M. Powell. 1980. Physical characteristics of human transferrin from small angle scattering. *Biophys. J.* 31:371–380.